



Cite this: *Chem. Commun.*, 2023, 59, 5051

Received 27th November 2022,  
Accepted 14th March 2023

DOI: 10.1039/d2cc06425a

[rsc.li/chemcomm](http://rsc.li/chemcomm)

**Peroxynitrite is a reactive oxygen and nitrogen species that participates in various biological reactions. Therefore, it is important to readily detect and track peroxynitrite in biological systems. Here, a novel turn-on probe encapsulated in PEG DSPE-PEG/HN-I was used to fluorescently detect  $\text{ONOO}^-$  rapidly. The encapsulation of HN-I using DSPE-PEG2000 optimizes the sensing performances of the naphthalimide probe and avoids ACQ. Using DSPE-PEG/HN-I to detect changes in the levels of exogenous  $\text{ONOO}^-$  in HepG2 cells and endogenous  $\text{ONOO}^-$  induced by LPS in RAW 267.4 cells was demonstrated.**

Peroxynitrite ( $\text{ONOO}^-$ ) is a short-lived bioactive agent, belonging to the category of reactive oxygen and nitrogen species (ROS/RNS). Peroxynitrite is an oxidant that generates free radicals, and acts as a Lewis base in living systems.<sup>1</sup> Upon exposure to peroxynitrite, biochemical cycles can be promoted while cellular function and viability may be adversely affected, depending on the concentrations of peroxynitrite.<sup>2</sup> Peroxynitrite at low

## Selective detection of peroxynitrite using an isatin receptor and a naphthalimide fluorophore†

Yueci Wu, <sup>‡</sup><sup>a</sup> Hai-Hao Han, <sup>‡</sup><sup>def</sup> Liu He, <sup>c</sup> Li Li, <sup>b</sup> Yi Zang, <sup>d</sup> Jia Li, <sup>‡</sup><sup>def</sup> Xiao-Peng He, <sup>\*c</sup> Yaping Ding, <sup>\*b</sup> Weiguo Cao <sup>\*b</sup> and Tony D. James <sup>\*ag</sup>

concentrations can contribute to programmed cell death while higher concentrations of peroxynitrite promote a disruption of cellular energy production resulting in necrotic cell death.<sup>3–5</sup> Peroxynitrite is involved in mediating numerous reactions, including the promotion of mitochondrial dysfunction, the regulation of cellular signalling pathways, the breaking of cellular redox status, and the induction of pain response under inflammatory conditions.<sup>6–10</sup> While, Hooper and Padalko have reported that peroxynitrite can mediate the immune response to virus infection.<sup>11,12</sup> However, due to a lack of rapid measurement tools suitable to detect peroxynitrite and quantify its concentrations *in vivo*, most of the biological reactions peroxynitrite participates in have only been investigated *in vitro*.<sup>2</sup> As such, in order to further explore the role of peroxynitrite in disease pathogenesis, it is necessary to investigate and develop effective methods for peroxynitrite detection.

Fluorescent probes can detect analytes based on changes in spectroscopic properties promoted by targeted reactions.<sup>13–15</sup> In general, a fluorescent probe consists of three units: a fluorophore that produces spectroscopic signals; a receptor that is able to react with a specific analyte; a linker that is suitable for connecting the fluorophore with the receptor.<sup>13,16,17</sup> According to the reaction between the receptor and the targeted analyte, a fluorescent probe can exhibit specified fluorescence responsiveness to its targeted analyte.<sup>18</sup> In addition, turn-on fluorescent probes can exhibit enhanced monitoring capabilities against dark backgrounds, which results in reduced background interference.<sup>18</sup>

Aryl boronate groups and  $\alpha$ -ketoamide groups have been widely applied in the design of peroxynitrite targeting probes due to their good sensitivity and rapid response.<sup>19</sup> However, these receptors can also react with other ROS species, such as hydrogen peroxide and hypochlorite.<sup>20–24</sup> Significantly, isatin exhibits a sensitive, selective and rapid response to peroxynitrite.<sup>25–28</sup>

Naphthalimide fluorophores are on the whole cell permeable and exhibit good photostabilities.<sup>29</sup> Due to the electron-withdrawing ability of its imide core, naphthalimide exhibits strong intramolecular charge transfer (ICT) in its solution state when the C-4 site of naphthalimide is modified by electron

<sup>a</sup> Department of Chemistry, University of Bath, Bath, BA2 7AY, UK.

E-mail: [t.d.james@bath.ac.uk](mailto:t.d.james@bath.ac.uk)

<sup>b</sup> Department of Chemistry, Shanghai University, Shanghai 200444, China.

E-mail: [wgcao@shu.edu.cn](mailto:wgcao@shu.edu.cn)

<sup>c</sup> Key Laboratory for Advanced Materials and Joint International Research

Laboratory of Precision Chemistry and Molecular Engineering, Feringa Nobel Prize Scientist Joint Research Center, Frontiers Center for Materiobiology and Dynamic Chemistry, School of Chemistry and Molecular Engineering, East China University of Science and Technology, 130 Meilong Rd, Shanghai 200237, China.

E-mail: [xphe@ecust.edu.cn](mailto:xphe@ecust.edu.cn)

<sup>d</sup> State Key Laboratory of Drug Research, Molecular Imaging Center, Shanghai Institute of Materia Medica, Chinese Academy of Sciences, Shanghai 201203, China. E-mail: [jli@simm.ac.cn](mailto:jli@simm.ac.cn)

<sup>e</sup> University of Chinese Academy of Sciences, No. 19A Yuquan Road, Beijing, 100049, China

<sup>f</sup> Shandong Laboratory of Yantai Drug Discovery, Bohai Rim Advanced Research Institute for Drug Discovery, Yantai, Shandong 264117, China

<sup>g</sup> School of Chemistry and Chemical Engineering, Henan Normal University, Xinxiang 453007, China

† Electronic supplementary information (ESI) available. See DOI: <https://doi.org/10.1039/d2cc06425a>

‡ These authors contributed equally.



donors.<sup>30–32</sup> These properties make naphthalimide an excellent fluorophore candidate for the construction of chemiluminescent probes for analyte detection in biological systems.<sup>30,33–37</sup> However, one of the main drawbacks of naphthalimide-based systems is low solubility. Poor solubility and the planar structure make naphthalimide undergo  $\pi$ - $\pi$  stacking easily, which results in aggregation-caused quenching (ACQ).<sup>29,38,39</sup>

In most cases, structural modification is used to solve solubility problems and overcome the ACQ of naphthalimide-based fluorophores.<sup>40–42</sup> However, this approach requires additional time-consuming synthesis. Therefore, we decided to explore a much simpler approach and use PEG encapsulation to improve solubility.<sup>43,44</sup> Polyethylene glycol (PEG) is widely used in the field of drug delivery as an excipient to improve molecular solubility.<sup>45–47</sup> In addition, DSPE-PEG2000 (1,2-distearoyl-sn-glycero-3-phosphoethanolamine-poly (ethylene glycol)) can reduce aggregation, improve the stability of nanoparticles and increase the circulation times of molecules *in vivo*.<sup>47–49</sup>

Here, we selected 4-hydroxy-1,8-naphthalimide (**HN**) as the fluorophore and a 1-methylindoline-2,3-dione moiety as the receptor to construct a novel fluorescent probe **HN-I** for the detection of  $\text{ONOO}^-$ . According to the specific redox reaction between  $\text{ONOO}^-$  and 1-methylindoline-2,3-dione, the fluorophore **HN** is released (Scheme 1).<sup>32,50</sup> In order to ensure the improvement of water solubility and the reduction of ACQ effect, we used DSPE-PEG2000 to encapsulate the fluorescent probe **HN-I** (Scheme 1).

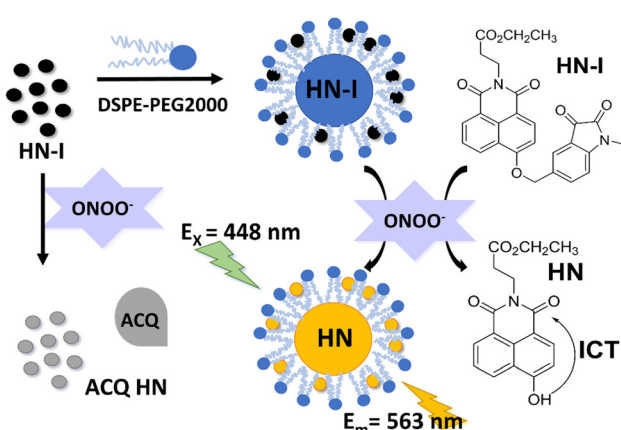
We were inspired by the group of Bruemmer who found that isatin-based groups could detect  $\text{ONOO}^-$  with high selectivities without any interference from other ROS/RNS.<sup>25</sup> As such, we prepared **HN** where the C-5 position of a 1-methylindoline-2,3-dione moiety was linked to a naphthalimide (Fig. S1, ESI†). Upon the addition of  $\text{ONOO}^-$ , the fluorescence of **HN-I** can be turned on (Fig. S2 and S3, ESI†). In addition, by using DSPE-PEG2000, the aqueous solubility of **DSPE-PEG/HN-I** can be improved. As we mentioned above, the improvement in solubility of **HN-I** when using DSPE-PEG2000 decreases the  $\pi$ - $\pi$  stacking of **HN-I**, which reduces ACQ and contributes to the recovery of the fluorescence (Fig. S4 and S5, ESI†). In other words, the sensing performances

of **DSPE-PEG/HN-I** were optimized by the encapsulation of DSPE-PEG2000 (Fig. S4 and S5, ESI† and Fig. 1a).

First, the absorption spectra of **DSPE-PEG/HN-I** were explored (Fig. 1a). Initially, the ICT effect of the probe was inhibited so that the probe was nonfluorescent. However, on the addition of  $\text{ONOO}^-$ , the naphthalimide fluorophore of **DSPE-PEG/HN** was released, and the recovery of the ICT effect resulted in fluorescence enhancement. As such, when the solution was excited at 448 nm, the fluorescence emission of **DSPE-PEG/HN** at 563 nm was enhanced. The fluorescence intensity of **DSPE-PEG/HN-I** increased with increasing concentrations of  $\text{ONOO}^-$  from 0  $\mu\text{M}$  to 30  $\mu\text{M}$  (Fig. 1b). For  $\text{ONOO}^-$  from 0–15  $\mu\text{M}$ , the fluorescence response was linear (Fig. 1c). The limit of the detection of **DSPE-PEG/HN-I** for  $\text{ONOO}^-$  was calculated to be 22 nM (Fig. 1c). The reaction rate between **DSPE-PEG/HN-I** and  $\text{ONOO}^-$  was rapid. From Fig. 1f, the fluorescence intensities reached the highest level at around 240 s. In addition, the selectivity of **DSPE-PEG/HN-I** was evaluated. Based on the graph of Fig. 1e, **DSPE-PEG/HN-I** exhibited no fluorescent responses upon the addition of other ROS including  $\text{ROO}^\bullet$ ,  $\text{H}_2\text{O}_2$ ,  $\text{O}_2^\bullet^-$ ,  $\cdot\text{OH}$ ,  ${}^1\text{O}_2$  and  $\text{ClO}^-$ . The pH sensitivity of **DSPE-PEG/HN-I** was then evaluated from 4.5 to 9.5 (Fig. 1d).<sup>9,51,52</sup> Over a pH range from 6.5 to 9.5, **DSPE-PEG/HN-I** exhibited low pH sensitivity, which confirms that **DSPE-PEG/HN-I** can be used for monitoring  $\text{ONOO}^-$  in biological systems.

Based on excellent sensing performances of **DSPE-PEG/HN-I** in solution, we evaluated **DSPE-PEG/HN-I** for imaging  $\text{ONOO}^-$  in a human liver cancer cell line (HepG2). Before cell fluorescence imaging tests, the cell viability of **DSPE-PEG/HN-I** was investigated in live HepG2 cells by a cell counting kit-8 (CCK-8) assay. The results suggested that **DSPE-PEG/HN-I** showed almost no cytotoxicity (cell viability  $\approx 100\%$  treated with a 40/40  $\mu\text{M}$  **DSPE-PEG/HN-I**) (Fig. S7, ESI†). **DSPE-PEG/HN-I** was evaluated with and without SIN-1 (a typical  $\text{ONOO}^-$  exogenous donor). As expected, without SIN-1, there was no fluorescence observed (Fig. 2a). However, with a concentration increase of SIN-1, the fluorescence intensity enhanced 5-fold (Fig. 2a–c). Then, **DSPE-PEG/HN-I** was also shown to detect exogenous  $\text{ONOO}^-$  in SIN-1-treated human cervical cancer cell line (HeLa). However, after pretreatment of cells with *N*-acetylcysteine (NAC, an  $\text{ONOO}^-$  scavenger), it attenuated the increase in the fluorescence of **DSPE-PEG/HN-I** induced by SIN-1 (Fig. S8, ESI†). Furthermore, the possibility of using **DSPE-PEG/HN-I** for endogenous  $\text{ONOO}^-$  detection was also investigated in a macrophage cell line (RAW 264.7). RAW 264.7 cells were incubated with lipopolysaccharide (LPS) which can promote inflammatory response and upregulate the concentration of  $\text{ONOO}^-$ .<sup>53–56</sup> As shown in Fig. 2D, the fluorescence intensity of **DSPE-PEG/HN-I** exhibited a 1.5-fold increase for LPS-loaded RAW 264.7 cells. After RAW 264.7 cells were incubated with both LPS and NAC, weak fluorescence was observed. All these results indicated that **DSPE-PEG/HN-I** can be applied for the detection of both exogenous and endogenous  $\text{ONOO}^-$ .

In summary, a novel turn-on probe was designed for the highly selective detection of  $\text{ONOO}^-$ . To avoid the ACQ effect, a disadvantage of naphthalimide fluorophores, DSPE-PEG2000 was used to encapsulate **HN-I** to improve the sensing performances.



Scheme 1 Schematic for use of **DSPE-PEG/HN-I** in the detection of peroxynitrite reaction mechanism of **HN-I**.



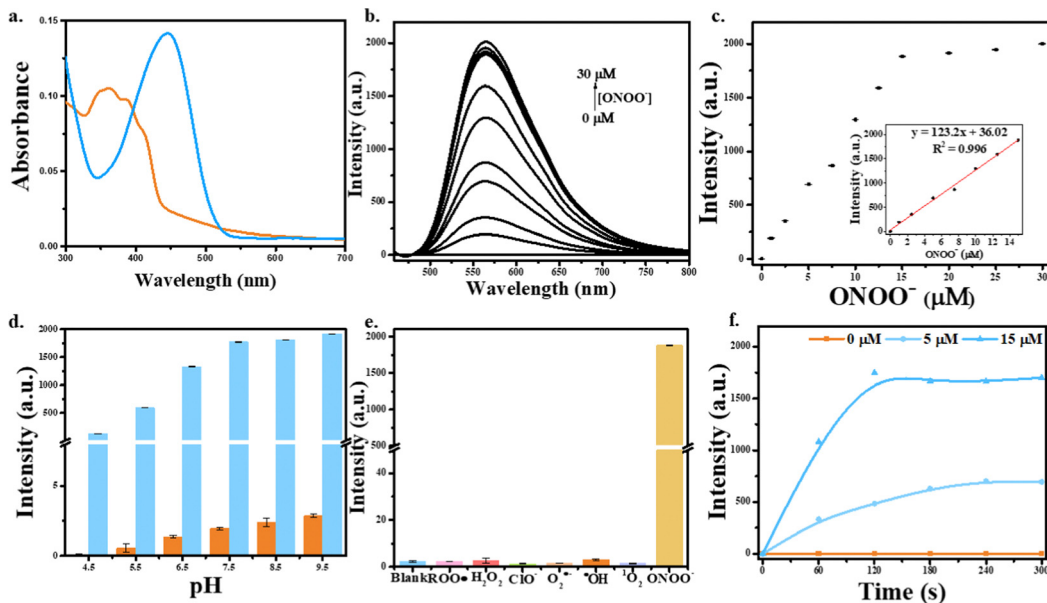


Fig. 1 (a) UV-vis of DSPE-PEG/HN-I (10/10  $\mu\text{M}$ ) without (the orange line) or with (the blue line) the addition of  $\text{ONOO}^-$  (30  $\mu\text{M}$ ). (b) Emission spectra for DSPE-PEG/HN-I (10/10  $\mu\text{M}$ ) in the presence of  $\text{ONOO}^-$  (0–30  $\mu\text{M}$ ). (c) Dose dependence curve at  $\lambda_{\text{max}} = 563$  nm. Inset: Linear fluorescence signals of DSPE-PEG/HN-I (10/10  $\mu\text{M}$ ) towards  $\text{ONOO}^-$  (0–15  $\mu\text{M}$ ). (d) Effects pH left on the fluorescence intensities of DSPE-PEG/HN-I (10/10  $\mu\text{M}$ ) without (red bars) or with (blue bars)  $\text{ONOO}^-$  (30  $\mu\text{M}$ ). (e) Selectivity data for Emission spectra for DSPE-PEG/HN-I (10/10  $\mu\text{M}$ ) upon the addition of  $\text{ONOO}^-$  (30  $\mu\text{M}$ ),  $\cdot\text{OH}$  (500  $\mu\text{M}$ ),  $\text{O}_2^-$  (500  $\mu\text{M}$ ),  $^1\text{O}_2$  (500  $\mu\text{M}$ ), and  $\text{ClO}^-$  (500  $\mu\text{M}$ ) after 5 min.  $\text{H}_2\text{O}_2$  (1 mM),  $\text{ROO}^\bullet$  (500  $\mu\text{M}$ ), and  $\text{ClO}^-$  (500  $\mu\text{M}$ ) were measured after 30 min. (f) The graph of time driver of DSPE-PEG/HN-I (10/10  $\mu\text{M}$ ) with the concentrations of  $\text{ONOO}^-$  at 0, 5, 15  $\mu\text{M}$ . The data was obtained in PBS buffer (5.5 mM, containing 1% DMSO),  $\text{pH} = 7.4$  at 25  $^\circ\text{C}$ ,  $\lambda_{\text{ex}} = 448$  nm,  $\lambda_{\text{em}} = 563$  nm.

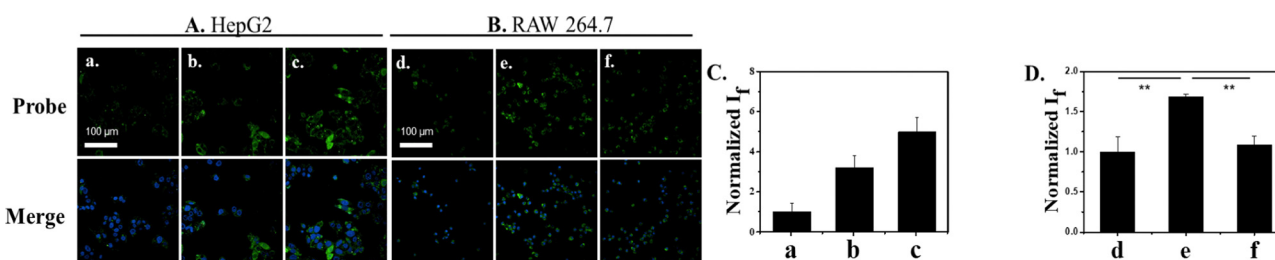


Fig. 2 (A) Imaging of exogenous  $\text{ONOO}^-$  in HepG2 cells. DSPE-PEG/HN-I (20/20  $\mu\text{M}$ , 1 h)-loaded HepG2 cells incubated with various concentration (a–c: 0, 2, 4 mM) of SIN-1 for 4 h, and then imaged. (B) Imaging of endogenous  $\text{ONOO}^-$  in RAW 264.7 cells. (d) RAW 264.7 cells incubated with 20/20  $\mu\text{M}$  DSPE-PEG/HN-I for 4 h and imaged. (e) RAW 264.7 cells were treated with  $1.0 \mu\text{g mL}^{-1}$  LPS for 24 h and incubated with 20/20  $\mu\text{M}$  DSPE-PEG/HN-I for 1 h and imaged. (f) RAW 264.7 cells were treated with  $1.0 \mu\text{g mL}^{-1}$  LPS for 24 h in the presence of 1 mM NAC and incubated with 20/20  $\mu\text{M}$  DSPE-PEG/HN-I for 1 h, and then imaged. Normalized intensities in a–c (C) and image d–f (D).  $\lambda_{\text{ex}} = 488$  nm,  $\lambda_{\text{em}} = 500$ –550 nm. In these cellular experiments, DMSO was used at the concentration of 0.2%.

We determined that DSPE-PEG/HN-I can detect  $\text{ONOO}^-$  rapidly in solution. In addition, DSPE-PEG/HN-I can be used to image exogenous and endogenous  $\text{ONOO}^-$ . These results confirm the potential of the DSPE-PEG/HN-I for the monitoring of  $\text{ONOO}^-$  in biological systems.

Y. W wishes to thank China Scholarship Council, the University of Bath and Shanghai University. TDJ wishes to thank the Royal Society for a Wolfson Research Merit Award and the Open Research Fund of the School of Chemistry and Chemical Engineering, Henan Normal University for support (2020ZD01). X.-P. H. thanks the National Natural Science Foundation of China (No. 21788102, 91853201 and 9185920077). J. L. and Y. Z. thank the National Natural Science Foundation of China (No. 82130099, 82151219, 31871414 and 81971265) and the

Shanghai Municipal Science and Technology Major Project (No. 22ZR1415200). H.-H. H. thanks the National Natural Science Foundation of China (No. 22107029) and Project funded by the China Postdoctoral Science Foundation (No. 2020M681196).

## Conflicts of interest

There are no conflicts to declare.

## Notes and references

- 1 G. Ferrer-Sueta, N. Campolo, M. Trujillo, S. Bartesaghi, S. Carballa, N. Romero, B. Alvarez and R. Radi, *Chem. Rev.*, 2018, **118**(3), 1338–1408.

2 C. Szabo, H. Ischiropoulos and R. Radi, *Nat. Rev. Drug Discovery*, 2007, **6**, 662–680.

3 C. Szabo, *Toxicol. Lett.*, 2003, **140**, 105–112.

4 P. Jagtap and C. Szabo, *Nat. Rev. Drug Discovery*, 2005, **4**, 421–440.

5 L. Virág, E. Szabo, P. Gergely and C. Szabo, *Toxicol. Lett.*, 2003, **140**, 113–124.

6 N. Nin, A. Cassina, J. Boggia, E. Alfonso, H. Botti, G. Peluffo, A. Trostchansky, C. Batthyany, R. Radi, H. Rubbo and F. J. Hurtado, *Intensive Care Med.*, 2004, **30**, 2271–2278.

7 A. L. Levonen, R. P. Patel, P. Brookes, Y. M. Go, H. Jo, S. Parthasarathy, P. G. Anderson and V. M. Darley-Usmar, *Antioxid. Redox Signaling*, 2001, **3**, 215–229.

8 D. Salvemini, T. M. Doyle and S. Cuzzocrea, *Biochem. Soc. Trans.*, 2006, **34**, 965–970.

9 R. Radi, *J. Biol. Chem.*, 2013, **288**, 26464–26472.

10 P. Pacher, J. Beckman and L. Liaudet, *Physiol. Rev.*, 2007, **87**, 315–424.

11 D. C. Hooper, R. B. Kean, G. S. Scott, S. V. Spitsin, T. Mikheeva, K. Morimoto, M. Bette, A. M. Rohrenbeck, B. Dietzschold and E. Weihe, *J. Immunol.*, 2001, **167**, 3470–3477.

12 E. Padalko, T. Ohnishi, K. Matsushita, H. Sun, K. Fox-Talbot, C. Bao, W. M. Baldwin and C. J. Lowenstein, *Proc. Natl. Acad. Sci. U. S. A.*, 2004, **101**, 11731–11736.

13 X. H. Li, X. H. Gao, W. Shi and H. M. Ma, *Chem. Rev.*, 2014, **114**, 590–659.

14 H. H. Han, H. Tian, Y. Zang, A. C. Sedgwick, J. Li, J. L. Sessler, X. P. He and T. D. James, *Chem. Soc. Rev.*, 2021, **50**, 9391–9429.

15 W. T. Dou, H. H. Han, A. C. Sedgwick, G. B. Zhu, Y. Zang, X. R. Yang, J. Yoon, T. D. James, J. Li and X. P. He, *Sci. Bull.*, 2022, **67**, 853–878.

16 A. P. de Silva, H. Q. N. Gunaratne, T. Gunnlaugsson, A. J. M. Huxley, C. P. McCoy, J. T. Rademacher and T. E. Rice, *Chem. Rev.*, 1997, **97**, 1515–1566.

17 W. Shi and H. M. Ma, *Chem. Commun.*, 2012, **48**, 8732–8744.

18 T. Ueno and T. Nagano, *Nat. Methods*, 2011, **8**, 642–645.

19 W. L. Cui, M. H. Wang, Y. H. Yang, J. Y. Wang, X. Z. Zhu, H. T. Zhang and X. X. Ji, *Coord. Chem. Rev.*, 2023, **474**, 214848.

20 J. W. Chen, T. C. Wu, W. Liang, J. J. Ciou and C. H. Lai, *Drug Delivery Transl. Res.*, 2022, DOI: [10.1007/s13346-022-01248-w](https://doi.org/10.1007/s13346-022-01248-w).

21 D. H. Tian, J. R. Liu, S. Y. Wang, S. Yan, Z. H. Chai, F. Dai, S. X. Zhang and B. Zhou, *Sens. Actuators, B*, 2022, **368**, 132149.

22 L. Zhen, J. S. Lan, S. A. Zhang, L. Liu, R. F. Zeng, Y. Chen and Y. Ding, *Anal. Methods*, 2022, **14**, 2147–2152.

23 X. L. Xie, X. E. Yang, T. H. Wu, Y. Li, M. M. Li, Q. Tan, X. Wang and B. Tang, *Anal. Chem.*, 2016, **88**, 8019–8025.

24 W. Shu, Y. L. Wu, S. P. Zang, S. Su, H. Kang, J. Jing and X. L. Zhang, *Sens. Actuators, B*, 2020, **303**, 127284.

25 K. J. Bruemmer, S. Merrikhahghi, C. T. Lollar, S. N. S. Morris, J. H. Bauer and A. R. Lippert, *Chem. Commun.*, 2014, **50**, 12311–12314.

26 X. Y. Lu, H. H. Su, J. Zhang, N. N. Wang, H. Wang, J. Y. Liu and W. L. Zhao, *Spectrochim. Acta, Part A*, 2022, **267**, 120537.

27 J. H. Xiong, W. W. Wang, C. X. Wang, C. Zhong, R. Q. Ruan, Z. Q. Mao and Z. H. Liu, *ACS Sens.*, 2020, **5**, 3237–3245.

28 W. W. Wang, J. H. Xiong, X. J. Song, Z. Wang, F. Zhang and Z. Q. Mao, *Anal. Chem.*, 2020, **92**, 13305–13312.

29 S. Mukherjee and P. Thilagar, *Chem. – Eur. J.*, 2014, **20**, 8012–8023.

30 S. A. Choi, C. S. Park, O. S. Kwon, H. K. Giong, J. S. Lee, T. H. Ha and C. S. Lee, *Sci. Rep.*, 2016, **6**(1), 26203.

31 S. U. Hettiarachchi, B. Prasai and R. L. McCarley, *J. Am. Chem. Soc.*, 2014, **136**, 7575–7578.

32 X. Lv, G. B. Ge, L. Feng, J. Troberg, L. H. Hu, J. Hou, H. L. Cheng, P. Wang, Z. M. Liu, M. Finel, J. N. Cui and L. Yang, *Bios. Bioelectron.*, 2015, **72**, 261–267.

33 R. K. Jackson, Y. Shi, X. D. Yao and S. C. Burdette, *Dalton Trans.*, 2010, **39**, 4155–4161.

34 A. P. de Silva, A. Goligher, H. Q. N. Gunaratne and T. E. Rice, *ARKIVOC*, 2003, **7**, 229–243.

35 A. P. de Silva and T. E. Rice, *Chem. Commun.*, 1999, 163–164.

36 L. Ingrassia, F. Lefranc, R. Kiss and T. Mijatovic, *Curr. Med. Chem.*, 2009, **16**, 1192–1213.

37 J. Liu, S. L. Zhong, L. L. Zhang, M. W. Yi, X. J. Liu, T. Bing, N. Zhang and D. H. Shangguan, *Chem. Commun.*, 2021, **57**, 6558–6561.

38 J. Gierschner, L. Luer, B. Milian-Medina, D. Oelkrug and H. J. Egelhaaf, *J. Phys. Chem. Lett.*, 2013, **4**, 2686–2697.

39 D. L. Reger, J. D. Elgin, R. F. Semeniuc, P. J. Pellechia and M. D. Smith, *Chem. Commun.*, 2005, 4068–4070.

40 C. G. Xu, T. Wu, L. Z. Duan and Y. M. Zhou, *Chem. Commun.*, 2021, **57**, 11366–11369.

41 S. Sharma, S. Srinivas, S. Rakshit and S. Sengupta, *Org. Biomol. Chem.*, 2022, **20**, 9422–9430.

42 J. Y. Zheng, J. Cao, Y. J. Tu, C. P. Huang, M. M. Liu and M. J. Zhang, *J. Mol. Struct.*, 2022, **1250**, 131868.

43 H. H. Han, A. C. Sedgwick, Y. Shang, N. Li, T. T. Liu, B. H. Li, K. Q. Yu, Y. Zang, J. T. Brewster, M. L. Odyniec, M. Weber, S. D. Bull, J. Li, J. L. Sessler, T. D. James, X. P. He and H. Tian, *Chem. Sci.*, 2020, **11**, 1107–1113.

44 L. Li, Z. M. Lin, X. C. Lu, C. Chen, A. Q. Xie, Y. P. Tang and Z. Q. Zhang, *RSC Adv.*, 2022, **12**, 33358–33364.

45 K. Knop, R. Hoogenboom, D. Fischer and U. S. Schubert, *Angew. Chem., Int. Ed.*, 2010, **49**, 6288–6308.

46 R. G. Strickley, *Pharm. Res.*, 2004, **21**, 201–230.

47 J. Che, C. I. Okeke, Z. B. Hu and J. Xu, *Curr. Pharm. Des.*, 2015, **21**, 1598–1605.

48 S. Y. Geng, B. Yang, G. W. Wang, G. Qin, S. Wada and J. Y. Wang, *Nanotechnology*, 2014, **25**, 275103.

49 N. O. Knudsen, S. Ronholt, R. D. Salte, L. Jorgensen, T. Thormann, L. H. Basse, J. Hansen, S. Frokjaer and C. Foged, *Eur. J. Pharm. Biopharm.*, 2012, **81**, 532–539.

50 J. Cao, W. W. An, A. G. Reeves and A. R. Lippert, *Chem. Sci.*, 2018, **9**, 2552–2558.

51 A. Denicola, J. M. Souza and R. Radi, *Proc. Natl. Acad. Sci. U. S. A.*, 1998, **95**, 3566–3571.

52 J. P. Crow, C. Spruell, J. Chen, C. Gunn, H. Ischiropoulos, M. Tsai, C. D. Smith, R. Radi, W. H. Koppenol and J. S. Beckman, *Free Radical Biol. Med.*, 1994, **16**, 331–338.

53 A. Kumar, S. H. Chen, M. B. Kadiiska, J. S. Hong, J. Zielonka, B. Kalyanaraman and R. P. Mason, *Free Radical Biol. Med.*, 2014, **73**, 51–59.

54 H.-H. Han, H.-M. Wang, P. Jangili, M. Li, L. Wu, Y. Zang, A. C. Sedgwick, J. Li, X.-P. He, T. D. James and J. S. Kim, *Chem. Soc. Rev.*, 2023, **52**, 879–920.

55 M. Weber, H.-H. Han, B.-H. Li, M. L. Odyniec, C. E. F. Jarman, Y. Zang, S. D. Bull, A. B. Mackenzie, A. C. Sedgwick, J. Li, X.-P. He and T. D. James, *Chem. Sci.*, 2020, **11**, 8567–8571.

56 X.-L. Hu, H.-Q. Gan, F.-D. Meng, H.-H. Han, D.-T. Shi, S. Zhang, L. Zou, X.-P. He and T. D. James, *Front. Chem. Sci. Eng.*, 2022, **16**, 1425–1437.

